B-cell CLL/Lymphoma 10 (BCL10) Is Required for NF-κB Production by Both Canonical and Noncanonical Pathways and for NF-κB-inducing Kinase (NIK) Phosphorylation[*]

Sumit Bhattacharyya[‡], **Alip Borthakur**[‡], **Sangeeta Tyagi**[‡], **Ravinder Gill**[‡], **Mei Ling Chen**[§], **Pradeep K. Dudeja**[‡¶], **and Joanne K. Tobacman**[‡¶1]

From the Departments of [‡]*Medicine and* [§]*Anatomy and Cell Biology, University of Illinois at Chicago, Chicago, Illinois 60612 and the* [¶]*Jesse Brown Veterans Affairs Medical Center, Chicago, Illinois 60612*

B-cell CLL/lymphoma 10 (BCL10), the caspase recruitment domain (CARD)-containing protein involved in the etiology of the mucosa-associated lymphoid tissue (MALT) lymphomas, has been implicated in inflammatory processes in epithelial cells, as well as in immune cells. Experiments in this report indicate that BCL10 is required for activation of nuclear factor (NF)-κB by both canonical and noncanonical pathways, following stimulation by the sulfated polysaccharide carrageenan (CGN). In wild type and IκB-kinase (IKK)$\alpha^{-/-}$ mouse embryonic fibroblasts, increases in phospho-IκBα, nuclear NF-κB p65 (RelA) and p50, and KC, the mouse analog of human interleukin-8, were markedly reduced by silencing BCL10 or by exposure to the free radical scavenger Tempol. In IKK$\beta^{-/-}$ cells, BCL10 silencing, but not Tempol, reduced the CGN-induced increases in KC, phospho-NF-κB-inducing kinase (NIK), cytoplasmic NF-κB p100, and nuclear NF-κB p52 and RelB, suggesting a BCL10 requirement for activation of the noncanonical pathway. In NCM460 cells, derived from normal, human colonic epithelium, the CGN-induced increases in NF-κB family members, p65, p50, p52, and RelB, were inhibited by BCL10 silencing. Although enzyme-linked immunosorbent assay and confocal images demonstrated no change in total NIK following CGN, increases in phospho-NIK in the wild type, IKK$\beta^{-/-}$ and IKK$\alpha^{-/-}$ cells were inhibited by silencing BCL10. These findings indicate an upstream signaling role for BCL10, in addition to its effects on IKKγ, the regulatory component of the IKK signalosome, and a requirement for BCL10 in both canonical and noncanonical pathways of NF-κB activation. Also, the commonly used food additive carrageenan can be added to the short list of known activators of both pathways.

The importance of activation of B-cell lymphoma/CLL 10 (BCL10)[2] has been recognized previously in the mucosa-associated lymphoid tissue (MALT) lymphomas, in which translocations involving MALT1 lead to constitutive activation of BCL10 and NF-κB transcription (1, 2). Other reports have defined a critical role for BCL10 in the inflammatory cascade in epithelial cells, including activation by lysophosphatidic acid (3), G-protein-coupled receptor (4), and angiotensin II (5). In this report, we demonstrate that BCL10 was required for NF-κB activation by both canonical and noncanonical pathways, following stimulation by the sulfated polysaccharide carrageenan (CGN) in mouse embryonic fibroblasts and in human colonic epithelial cells. Previously, we reported that CGN significantly up-regulated transcription of BCL10 in NCM460 cells (6, 7).

The sulfated polysaccharide carrageenan has been widely used for decades to induce inflammation in animal and tissue culture models. In our previous work, CGN was shown to induce an inflammatory cascade in human colonic epithelial cells by two distinct mechanisms: an immune-mediated mechanism involving TLR4 (toll-like receptor 4), IRAK (IL-1β receptor activating kinase), BCL10, phospho-IκBα (inhibitor of κB), NF-κB (nuclear factor κB), and IL-8 (interleukin-8); and a reactive oxygen species (ROS)-mediated mechanism involving phospho-Hsp27, IκB kinase (IKK)-β, phospho-IκBα, BCL10, NF-κB, and IL-8 (6–9). Carrageenan activation of these pathways was attributable to its distinctive chemical structure, including its resemblance to the naturally occurring glycosaminoglycans, its highly sulfated galactose residues, and its unusual α-Gal(1→3)Gal bond that is a known immune epitope (10, 11). Because CGN is a commonly used food additive in the Western diet, these pathways may induce inflammation and disease in the human colon and implicate a role for BCL10 in human disease, in addition to the MALT lymphomas.

To further define the BCL10-mediated activation of NF-κB and the interactions between the ROS and TLR4-BCL10 pathways, the requirements for different components of the IKK signaling complex and the responses of different members of the NF-κB family were investigated. The IKK signaling complex, including the catalytic components IKKα and IKKβ and the regulatory component IKKγ, also known as NEMO (NF-κB essential modifying factor), integrates upstream signals and leads to the phosphorylation of IκBα. Subsequently, phospho-IκBα is ubiquitinated, and the localization signal for NF-κB nuclear translocation is exposed. These events represent critical signals in the progression of the inflammatory cascade from

[1] To whom correspondence should be addressed: University of Illinois at Chicago, Dept. of Medicine, 840 S. Wood St., M/C 718, 440 CSN, Chicago, IL 60612. Tel.: 312-569-7826; Fax: 312-413-8283; E-mail: jkt@uic.edu.
[2] The abbreviations used are: BCL10, B-cell lymphoma/CLL 10; CGN, carrageenan; WT, wild type; ELISA, enzyme-linked immunosorbent assay; ROS, reactive oxygen species; FACE, fast-activated cell-based; siRNA, small interfering RNA; NIK, NF-κB-inducing kinase; IKK, IκB kinase; SCBT, Santa Cruz Biotechnology, Inc.; MEF, mouse embryonic fibroblast.

a series of membrane events to a cellular reaction with transcriptional responses. To clarify the role of BCL10 with different components of the IKK signalosome and the subsequent effects on members of the NF-κB family, experiments with mouse embryonic fibroblasts that lack either IKKα or IKKβ were performed, and the inter-relationships among BCL10, phospho-NIK, and NF-κB family members, including p65, p100, p50, p52, RelB, and c-Rel, were determined.

EXPERIMENTAL PROCEDURES

NCM460 Cells and Mouse Embryonic Fibroblasts in Tissue Culture—NCM460 is a nontransfected human colonic epithelial cell line that was derived from the normal colonic mucosa of a 68-year-old Hispanic male (12). NCM460 cells were grown in M3:10^{TM} media (INCELL, San Antonio, TX) and maintained at 37 °C in a humidified, 5% CO_2 environment with media changes at 2-day intervals. Confluent cells were harvested by trypsinization, and subcultured in multiwell tissue culture clusters (Costar). Cells were treated with λ-carrageenan (CGN) 1 μg/ml (Sigma-Aldrich), for 1–24 h, and spent media were collected from control and treated wells and stored at −80 °C. Cells were harvested by scraping. Total cell protein was measured by BCA^{TM} protein assay kit (Pierce), using bovine serum albumin as standard.

Mouse embryonic fibroblasts, including wild type (WT), IKKα$^{−/−}$, and IKKβ$^{−/−}$ were a generous gift from the laboratory of Dr. Michael Karin (University of California, San Diego). These cell lines were obtained from transgenic mice in which IKKα and IKKβ genes were deleted and homozygous mice were bred (13, 14). Cells were grown in Dulbecco's modified Eagle's medium with 10% fetal bovine serum and treated as indicated above.

Superoxide Scavenger Tempol—The superoxide scavenger Tempol (4-hydroxy-2,2,6,6-tetramethyolpiperidinyloxy; Axxora, San Diego, CA) was used to inhibit the effects of free oxygen radicals generated by CGN. Tempol was used at a concentration of 100 nM and coadministered with CGN (1 μg/ml) for 24 h as described previously (8).

ELISAs for Measurement of Secreted IL-8 and KC and of Cellular BCL10 and Phospho-IκBα—The secretion of IL-8 in the spent medium of control and treated NCM460 cells was measured using the DuoSet ELISA kit for human IL-8 (R&D Systems, Minneapolis, MN), as described previously (9).

KC, the mouse homolog of IL-8, was measured by ELISA (R&D Systems) in spent medium, and the results were compared with standards. The sample values were normalized with the total cell protein concentrations determined by BCA^{TM} Protein assay kit (Pierce), and KC values were expressed as pg/mg protein.

Expression of BCL10 protein in control and CGN-treated NCM460 cells was determined by a solid-phase ELISA, previously developed by our laboratory for quantitative determination of BCL10 (15). Control or treated cells were lysed in RIPA buffer (50 mM Tris containing 0.15 M NaCl, 1% Nonidet P-40, 0.5% deoxycholic acid, and 0.1% SDS, pH 7.4), and the cell extracts were stored at −80 °C until assayed, using ELISA as reported previously (16).

Phospho-IκBα was determined using an ELISA assay in NCM460 cells and in mouse embryonic fibroblasts, including WT, IKKα$^{−/−}$, and IKKβ$^{−/−}$ cells, as described previously (6). IκBα phosphorylated at Ser^{32} was detected by the PathScan® Sandwich ELISA kit (Cell Signaling), which is a solid-phase sandwich ELISA with a mouse monoclonal antibody against IκBα coated onto the microwells of a 96-well plate.

FACE Assays for NIK and Phospho-NIK—Total and phospho-NIK in control and treated human cell samples were measured by a fast-activated cell-based (FACE) ELISA (Active Motif) (17) using a primary goat antibody for NIK (sc-7211; Santa Cruz Biotechnology, Santa Cruz, CA) against the epitope 700-947 and phospho-NIK (sc-12957; SCBT) that recognized Thr^{559}. Measurements of optical density were compared between control and treated samples.

FACE Assays for BCL10 and Phospho-BCL10—Specific antibody for phospho-BCL10 (Ser 138; SCBT) and BCL10 antibody (QED Biosciences Inc., San Diego, CA; epitope AA 5–19) were used to detect the content of phospho-BCL10 (Ser^{138}) and total BCL10 present in the NCM460 cells following exposure to λCGN (1 μg/ml for 24 h) and to compare with untreated control cells.

Determinations of NF-κB p65, p50, p52, RelB, c-Rel, and p100—Nuclear extracts were prepared from treated and control NCM460 cells as described previously, using a nuclear extraction kit (Active Motif, Carlsbad, CA). Activated NF-κB family members in the samples were determined by oligonucleotide-based ELISA (Active Motif). The specificity of the binding of NF-κB of the samples with the coated nucleotide sequence was determined by comparison to the control binding, determined by adding either free consensus nucleotide (5′-AGTTGAGGG-GACTTTCCCAGGC-3′) or mutated nucleotide (5′-AGTT-GAGGCCACTTTCCCAGGC-3′) to the reaction buffer, as described previously (17). The sample values were normalized with the total cell protein determined by protein assay kit (Pierce).

Co-immunoprecipitation of IKKγ with BCL10 and Ubiquitin—Cells treated with vehicle or carrageenan (1 μg/ml) for 24 h were washed in cold phosphate-buffered saline and lysed in a lysis buffer (20 mM Tris, pH 7.5, 150 mM NaCl, 1% Triton X-100, 1 mM Na$_2$EDTA, 1 mM EGTA, 1% Triton, 2.5 mM sodium pyrophosphate, 1 mM β-glycerophosphate, 1 mM Na$_3$VO$_4$, 1 μg/ml leupeptin) (Cell Signaling). The cell lysates were precleared with protein A/G plus-agarose (Santa Cruz Biotechnology) and then incubated with anti-ubiquitin antibody (SCBT) at 4 °C for 16 h, followed by incubation with protein A/G plus-agarose for 5 h. Parallel control experiments were performed by incubating the precleared cell lysate with normal rabbit IgG followed by incubation with protein A/G plus-agarose. The agarose beads were collected by centrifugation, washed four times with lysis buffer and heated to 95 °C for 5 min after adding Laemmli buffer. For the immunoblots, the resulting immunoprecipitates or the proteins in the nuclear extracts or in the whole cell lysates were separated by SDS-PAGE, transferred onto nitrocellulose membranes (Amersham Biosciences), and probed with the indicated human or mouse antibodies (anti-IKKγ, anti-ubiquitin, anti-NF-κB p100, or anti-BCL10; SCBT) and the immu-
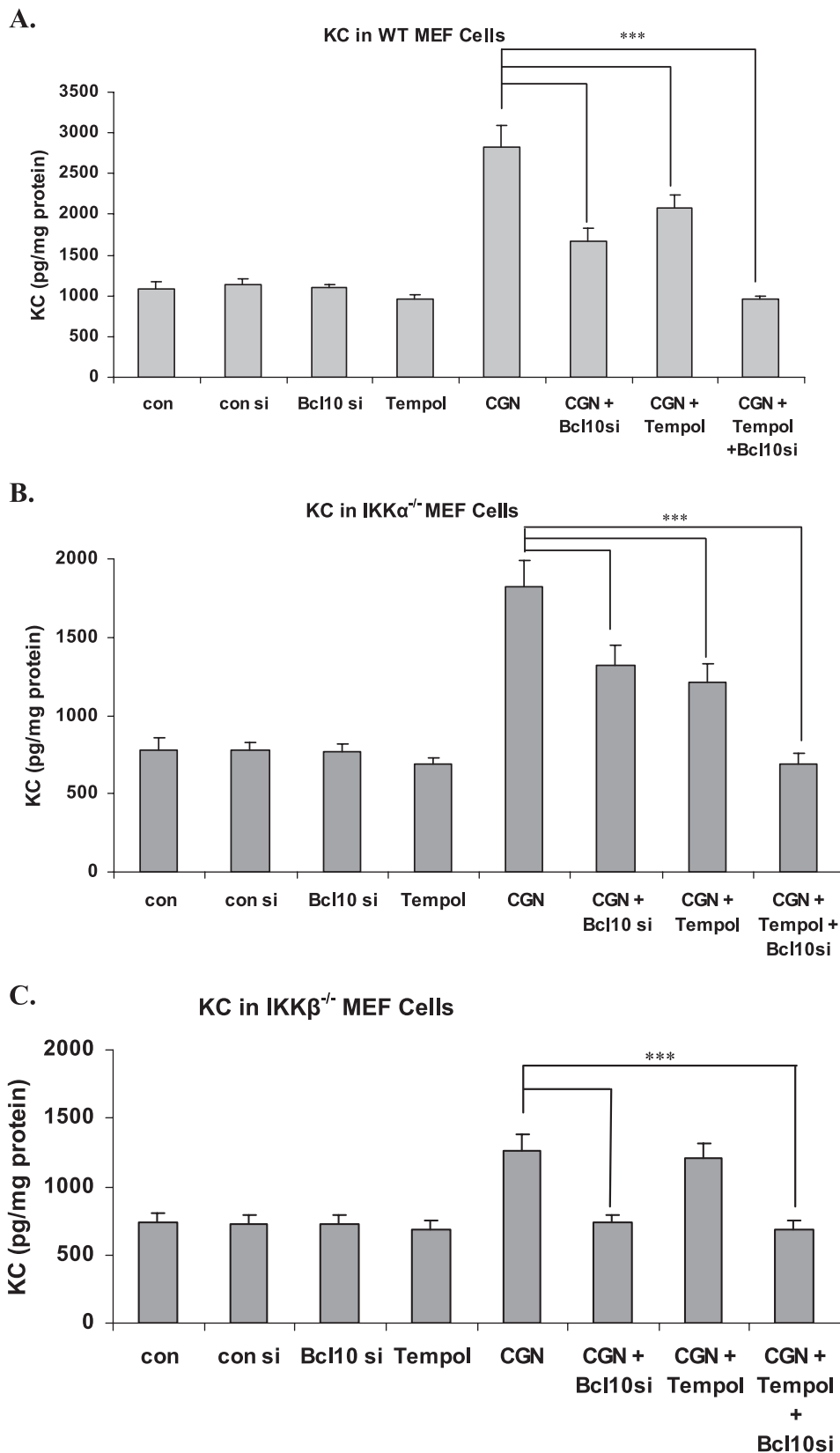
noreactive bands were visualized using enhanced chemilumi-nescence (Amersham Biosciences).

Confocal Microscopy of Phospho-NIK in NCM460 Cells—NCM460 cells were grown in compartment slides for 24 h until 50% confluent. Then, cells were treated with either control small interfering RNA (siRNA), BCL10 siRNA, or control $IgG_{2\alpha}$ antibody. After 24 h, test cells were exposed to λCGN (1 μg/ml) for 24 h. Methods for staining and examination of cells by confocal microscopy were described previously (9). Cells were washed once in 1× phosphate-buff-ered saline containing 1 mM calcium chloride, pH 7.4, fixed for 1.5 h with 2% paraformaldehyde, and then permeabilized with 0.08% saponin. Preparations were washed with phosphate-buffered saline, blocked in 5% normal goat serum, incubated overnight with NIK or phospho-NIK antibody at 4 °C, and then washed and stained with either Alexa Fluor® 568 donkey anti-goat or goat-anti-rabbit IgG (H+L) (1:100, Invitrogen). Cells were exposed for 1 h to Alexa Fluor® 488 phalloidin (Invitrogen) di-luted 1:40 to stain actin and cover-slipped using 4′,6-diamidino-2-phenylindole-mounting medium (Vectashield®, Vector Laboratories, Inc., Burlingame, CA) for nuclear staining. Preparations were washed thoroughly, mounted, and observed using a Zeiss LSM 510 laser scan-ning confocal microscope equipped with excitation at 488 and 534 nm from an Ar/Kr laser and at 361 nm from a UV laser. Green and red fluorescence were detected through LP505 and 585 filters. The fluorochromes were scanned sequentially, and the collected images were exported with Zeiss LSM Image Browser software as TIFF files for analysis and reproduction.

Silencing of BCL10 mRNA Expression—Silencing BCL10 was performed as described previously (6, 16). Effectiveness of BCL10 silencing in the NCM460 cells and the MEF was determined by BCL10 ELISA, following exposure to BCL10 siRNA for 24 h. In the NCM460 cells, silencing reduced

baseline BCL10 protein by ~82% (from 1.30 (±0.07) to 0.24 (±0.02) ng/mg protein). Bcl10 was reduced by ~81% in the WT MEF cells, but precise quantification was not possible due to a lack of mouse recombinant Bcl10.

A.

B.

C.

FIGURE 2. **NF-κB family members are affected differently by CGN exposure in the IKKα$^{-/-}$ and IKKβ$^{-/-}$ cells.** A, Western blot for p100 in MEF cells demonstrates no increase in the IKKα$^{-/-}$ cells, in contrast to changes in the IKKβ$^{-/-}$ and WT cells, in which p100 increases following CGN exposure and then declines following BCL10 silencing. Densitometric measurements demonstrate significant increases following CGN ($p < 0.001$) and significant declines when BCL10 was silenced ($p < 0.001$) in the WT and IKKβ$^{-/-}$ MEF cells, but not in the IKKα$^{-/-}$ MEF cells. B, in the WT cells, CGN exposure leads to significant increases in p65, p50, p52, and RelB, which are inhibited by BCL10 silencing ($p < 0.001$). C, in the IKKα$^{-/-}$ cells, no increases in p52 or RelB occur. The increases in p65 and p50 are significant and are reduced when BCL10 is silenced ($p < 0.001$). D, in the IKKβ$^{-/-}$ cells, no increases in p65 or p50 occur, and the increases in p52 and RelB are inhibited when BCL10 is silenced ($p < 0.001$). E, in the NCM460 cells, CGN exposure induced increases in p65, p50, p52, and RelB, but not c-Rel. These increases were inhibited when BCL10 was silenced ($p < 0.001$). Hence, silencing BCL10 consistently reduces the CGN-induced increases in NF-κB components.

RESULTS

BCL10 Silencing Reduced Increases of KC in WT, IKKα$^{-/-}$, and IKKβ$^{-/-}$ MEFs—Silencing BCL10 reduced the increases in KC that followed exposure to λCGN (1 μg/ml × 24 h) in the MEF cells, including WT (Fig. 1A), IKKα$^{-/-}$ (B), and IKKβ$^{-/-}$ (C). The ROS inhibitor Tempol also reduced the increase in KC in the IKKα$^{-/-}$ (IKKβ-containing) cells, but not in the IKKβ$^{-/-}$ (IKKα-containing) cells. The combination of BCL10 silencing and Tempol completely inhibited the increase in KC in the WT and IKKα$^{-/-}$ cells. KC increased by ~1.78 ng/mg protein in the WT cells, ~1.09 ng/mg protein in the IKKα$^{-/-}$ cells, and least (~0.50 ng/mg protein) in the IKKβ$^{-/-}$ cells, following CGN exposure.

Differences in BCL10 Protein Expression in the IKKα$^{-/-}$ and IKKβ$^{-/-}$ Cells—At baseline in the WT MEF, BCL10 cellular concentration was 2.05 (±0.17) ng/mg protein, increasing to 4.85 (±0.11) ng/mg protein following exposure to λCGN 1 μg/ml for 24 h (data not shown). In IKKα$^{-/-}$ cells following CGN exposure, BCL10 increased from 1.59 (±0.09) ng/mg protein to 3.78 (±0.33) ng/mg protein. In the IKKβ$^{-/-}$ cells, BCL10 increased from 1.74 (±0.18) ng/mg protein to 4.22 (±0.59) ng/mg protein following CGN. These results demonstrate ~2–3-fold increases in BCL10 protein expression following CGN exposure, and the response occurred in both IKKα and IKKβ cells, as well as the WT cells.

BCL10 Silencing Has Differential Effects on NF-κB Family Members in IKKα$^{-/-}$ and IKKβ$^{-/-}$ Cells—NF-κB components include p65 (RelA), RelB, and c-Rel, which have a transactivating domain, and p50 and p52, which are products of proteasomal degradation of p105 and p100, respectively. In the IKKβ$^{-/-}$ and WT MEF cells, BCL10 silencing markedly reduced the CGN-induced increases in p100, as
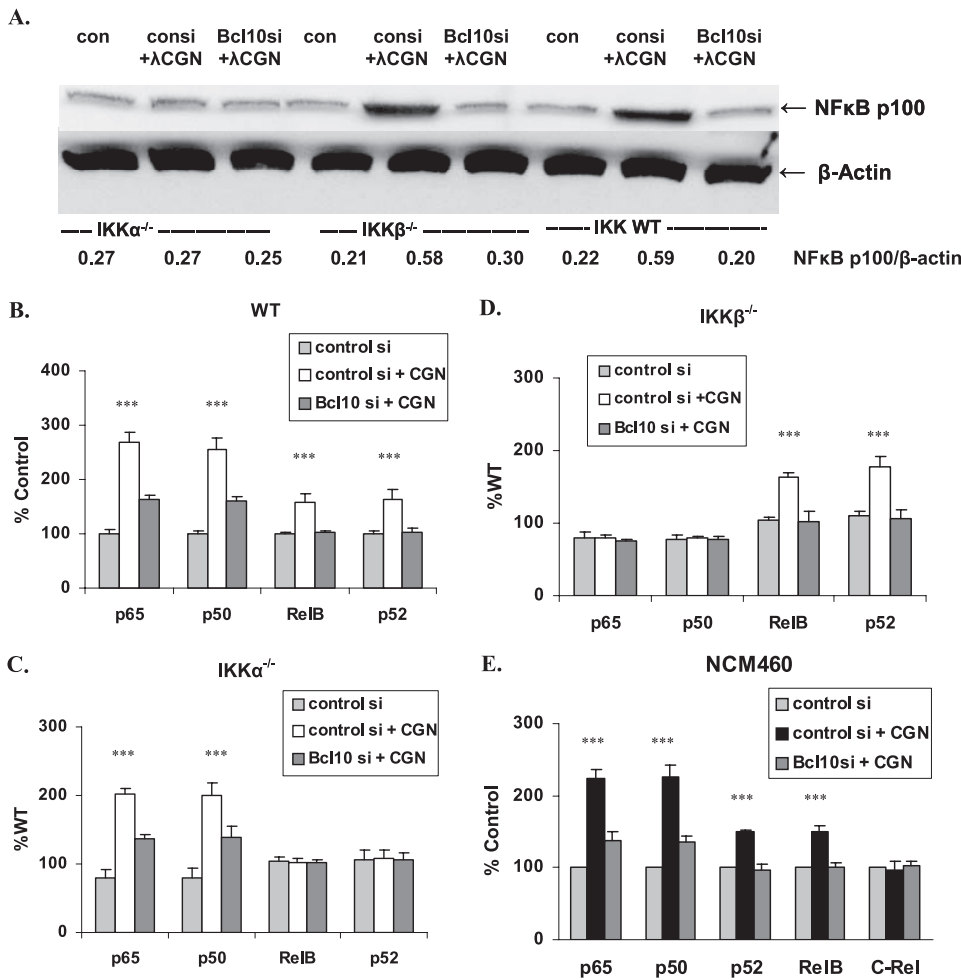
Statistical Analysis—Unless stated otherwise, statistical significance was determined by one-way analysis of variance, followed by post hoc Tukey-Kramer test for multiple comparisons using Instat software. Measurements are the mean of at least three independent biological experiments with technical replicates ± S.D. A p value <0.05 was considered statistically significant. One asterisk indicates statistical significance at the $0.01 < p \leq 0.05$ level, two asterisks $0.001 < p \leq 0.01$, and three asterisks, $p \leq 0.001$. Error bars designate S.D.

FIGURE 1. **KC increase in MEF cells is inhibited by Tempol in WT and IKKα$^{-/-}$ cells, but not in the absence of IKKβ.** A, KC, the mouse homolog of IL-8, increased in the WT MEF cells after exposure to CGN. This increase was reduced by either combined exposure with the free radical scavenger Tempol (100 nM for 24 h) or silencing by BCL10 siRNA. The combination of Tempol and BCL10 silencing completely inhibited the increase in KC ($p < 0.001$). B, similar responses occurred in the IKKα$^{-/-}$ cells ($p < 0.001$). C, in contrast, in the IKKβ$^{-/-}$ cells, Tempol had no effect on KC secretion, demonstrating that the IKKα-mediated pathway is independent of ROS, but requires BCL10. All figures are based on at least three biological replicates with technical noduplicates of each measurement. ***, $p < 0.001$. si, small interfering RNA; con, control.
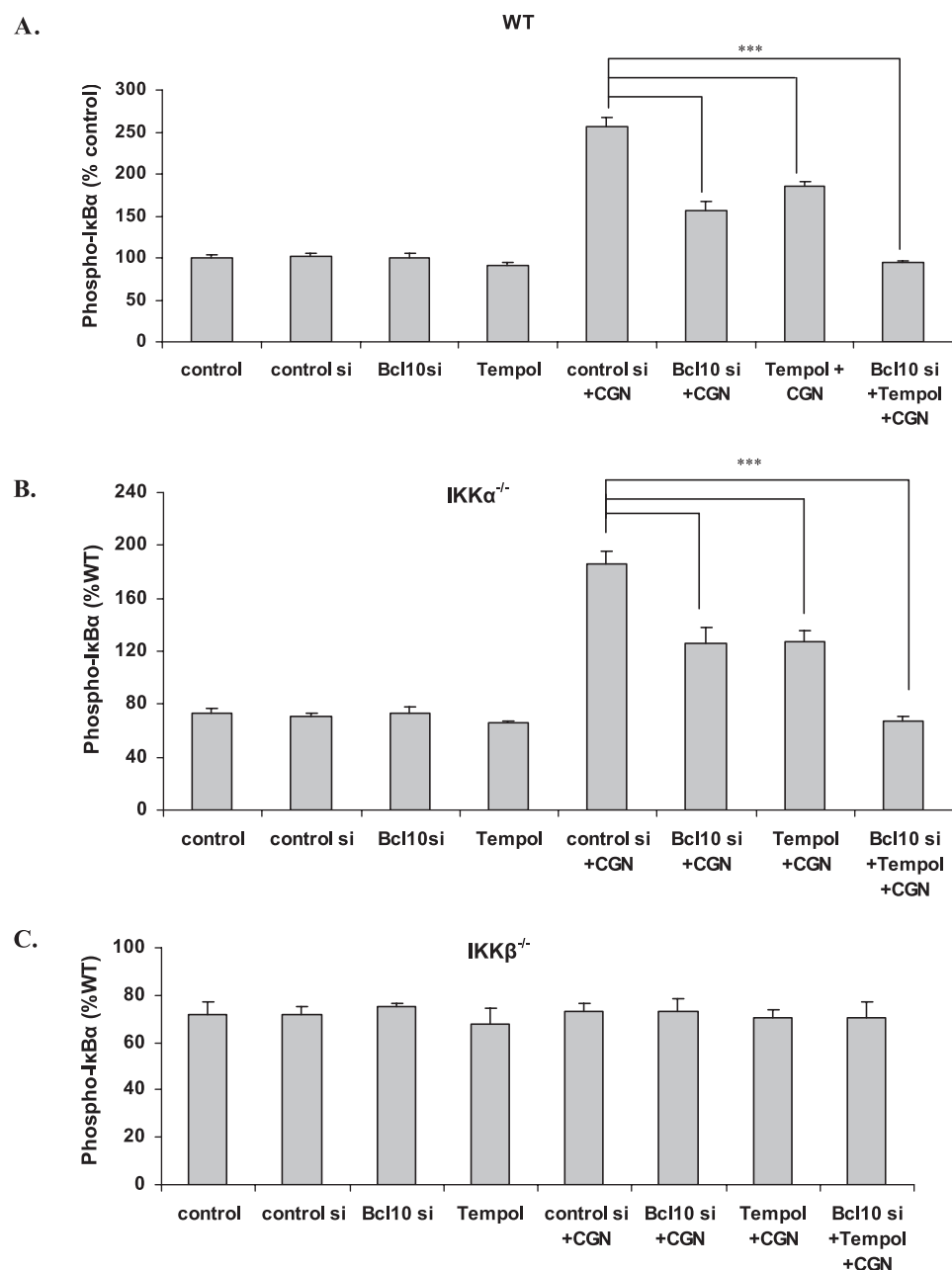
FIGURE 3. **Differential increases in phospho-IκBα in the MEF IKKα$^{-/-}$ and β$^{-/-}$ cells.** *A*, in the MEF WT cells, the CGN-induced increases in phospho-IκBα were reduced by Tempol and by BCL10 silencing ($p < 0.001$). *B*, results were similar in the IKKα$^{-/-}$ cells ($p < 0.001$). *C*, in contrast, in the IKKβ$^{-/-}$ cells, phospho-IκBα did not increase following CGN exposure.

pletely abrogated the increases in p52 and RelB and significantly reduced the increases in p65 and p50 (Fig. 2*E*). BCL10 silencing had no effect on c-Rel.

CGN Exposure Increases and BCL10 Silencing Reduces Phospho-IκBα in WT and IKKα$^{-/-}$ Cells, but Not in IKKβ$^{-/-}$ Cells—When WT (Fig. 3*A*) or IKKα$^{-/-}$ (*B*) cells, were exposed to CGN, phospho-IκBα production increased to 2.6 times the baseline. These increases were reduced by Tempol or by BCL10 silencing, and completely inhibited by their combination. In the IKKβ$^{-/-}$ cells (Fig. 3*C*), phospho-IκBα did not increase following CGN exposure. These results are consistent with CGN induction through IKKα of a phospho-IκBα independent pathway of NF-κB activation.

BCL10 Required for CGN-induced Increases in Phospho-NIK in MEF and NCM460 Cells—In the MEF and NCM460 cells, no significant changes in total NIK followed CGN treatment (Fig. 4, *A–D*). However, following CGN, phospho-NIK, increased in the WT (Fig. 4*A*) to 2.5× the baseline, in IKKα$^{-/-}$ to 3.1× the baseline (*B*), in the IKKB$^{-/-}$ (*C*) cells to 2.3× the baseline and in the NCM460 cells to 2.2× the baseline (*D*), as measured by the FACE assay. BCL10 silencing blocked these increases, demonstrating a requirement for BCL10 to phosphorylate NIK following CGN exposure.

Increased Phospho-BCL10 (Ser^{138}) following CGN in NCM460 Cells—CGN exposure produced a 4-fold increase ($n = 6$, $p < 0.001$) in phospho(Ser^{138})-BCL10, compared with baseline in the NCM460 cells, when measured by FACE assay. Because BCL10 was required for NIK phosphorylation, the findings suggest that activation of BCL10 by phosphorylation preceded NIK phosphorylation and was independent of IKKα and IKKβ in these experiments. In contrast, tumor necrosis factor-α-induced NIK phosphorylation was found to be independent of BCL10 (data not shown).

Images by confocal microscopy of total NIK (Fig. 5, *A–F*) and phospho-NIK (*G–M*) in NCM460 cells support the finding that CGN-induced NIK phosphorylation is dependent on BCL10. Total NIK images demonstrate diffuse cytoplasmic, as well as membrane localization of NIK in the untreated control (Fig. 5, *A–B*). Staining intensity did not increase following CGN either

detected by Western blot and by densitometry (Fig. 2*A*). Consistent with this, the CGN-induced increases of nuclear p52 shown by ELISA in the WT and IKKβ$^{-/-}$ cells declined when BCL10 was silenced, but with no change in the IKKα$^{-/-}$ cells (Fig. 2, *B–D*).

In the WT MEF cells, CGN exposure produced significant increases in p65, p50, p52, and RelB (Fig. 2*B*). In the IKKα$^{-/-}$ cells, p52 and RelB did not increase (Fig. 2*C*), and in the IKKβ$^{-/-}$ cells, p65 and p50 did not increase (*D*). BCL10 silencing completely reduced the increases in p52 and RelB and significantly reduced the declines in p65 and p50.

In NCM460 cells, CGN exposure produced increases in p65, p50, p52, RelB, but not c-Rel. Again, BCL10 silencing com-
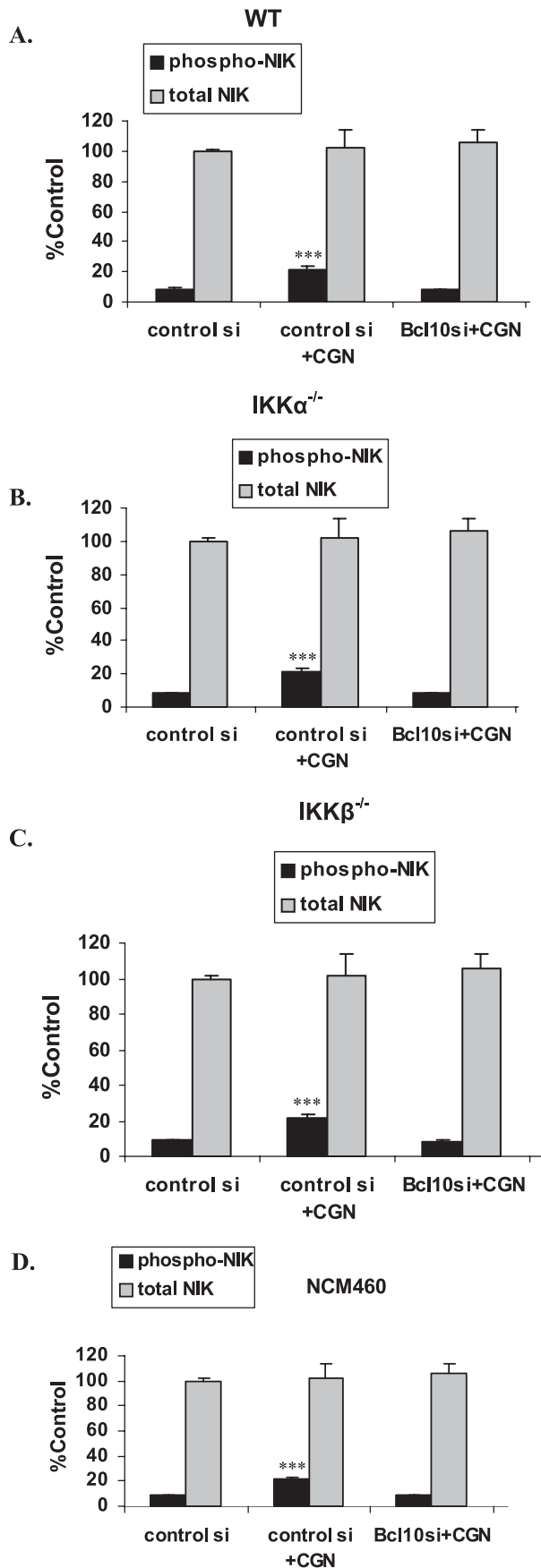
A.

WT

B.

IKKα$^{-/-}$

C.

IKKβ$^{-/-}$

D.

NCM460

in the presence of control siRNA (Fig. 5, *C–D*) or BCL10 siRNA (*E–F*). An increase in membrane-associated NIK staining is seen following CGN with control siRNA, but not with BCL10 siRNA treatment. When fluorescent immunostaining with phospho-NIK was performed and confocal images were acquired, no phospho-NIK was seen in the untreated control (Fig. 5, *G–H*) or following BCL10 siRNA (*K–L*), in contrast to the appearance following CGN exposure in the presence of control siRNA (*I–J*). The presence of cell membrane-associated phospho-NIK is demonstrated in the z-stack images (Fig. 5*M*), in which phospho-NIK immunostaining appeared only along the outer membrane of NCM460 cells and did not penetrate to the interior of the cells.

IKKγ Co-immunoprecipitated with BCL10 and IKKγ Ubiquitination Increased following CGN in NCM460 Cells—Following NCM460 cell treatment with CGN, immunoprecipitation with ubiquitin and Western blot with IKKγ were performed. Increase in ubiquitinated IKKγ was apparent, with increased density of the higher molecular mass band and reduction in density of the baseline IKKγ band (Fig. 6*A*). Also, IKKγ co-immunoprecipitated with BCL10 in the NCM460 cells, and the BCL10 that co-immunoprecipitated with the IKKγ increased in response to CGN (Fig. 6*B*). These findings demonstrate that in addition to the observed effects of BCL10 and CGN on the catalytic components IKKα and IKKβ of the IKK signalosome, there is also an impact on the ubiquitination of IKKγ, the regulatory component of the IKK signalosome.

DISCUSSION

BCL10 emerges as an important mediator of both the canonical and noncanonical pathways of NF-κB activation stimulated by CGN in NCM460 cells and MEF (Fig. 7). BCL10 was increased by CGN in both IKKα$^{-/-}$ and IKKβ$^{-/-}$ MEF, and BCL10 silencing by siRNA reduced CGN-induced stimulation of p65, p50, p100, p52, and RelB in MEF and NCM460 cells. These effects implicate BCL10 in the inflammatory cascade beyond its interaction with IKKγ and emphasize that BCL10 has a key role as a mediator of the innate immune response in epithelial, as well as its more established role in immune cells (18, 19).

Unexpectedly, the studies presented in this report revealed that CGN stimulated both the noncanonical, as well as the canonical pathway of NF-κB activation and that BCL10 was required for these effects upstream of the IKK signalosome. CGN joins the small group of known mediators of both the noncanonical and canonical pathways that includes lymphotoxin and B-cell activating factor (20, 21).

FIGURE 4. **CGN-induced increases in phospho-NIK are inhibited by BCL10 silencing.** Phospho-NIK and total NIK were measured by FACE assay using antibodies for phospho-NIK (Thr^{559}) and total NIK. *A*, in the MEF cells, no changes in total NIK followed CGN treatment. Following CGN, phospho-NIK increased significantly in the WT cells ($p < 0.001$). The CGN-induced increases in phospho-NIK were inhibited by BCL10 silencing. *B*, similar effects were found in the IKKα$^{-/-}$ cells ($p < 0.001$ for phospho-NIK increase). *C*, in the IKKβ$^{-/-}$ cells, similar responses were detected ($p < 0.001$ for phospho-NIK increase). *D*, similarly, in the NCM460 cells, CGN produced an increase of ~11% in phospho-NIK ($p < 0.001$). These findings demonstrate a requirement for BCL10 for the phosphorylation of NIK following CGN exposure.
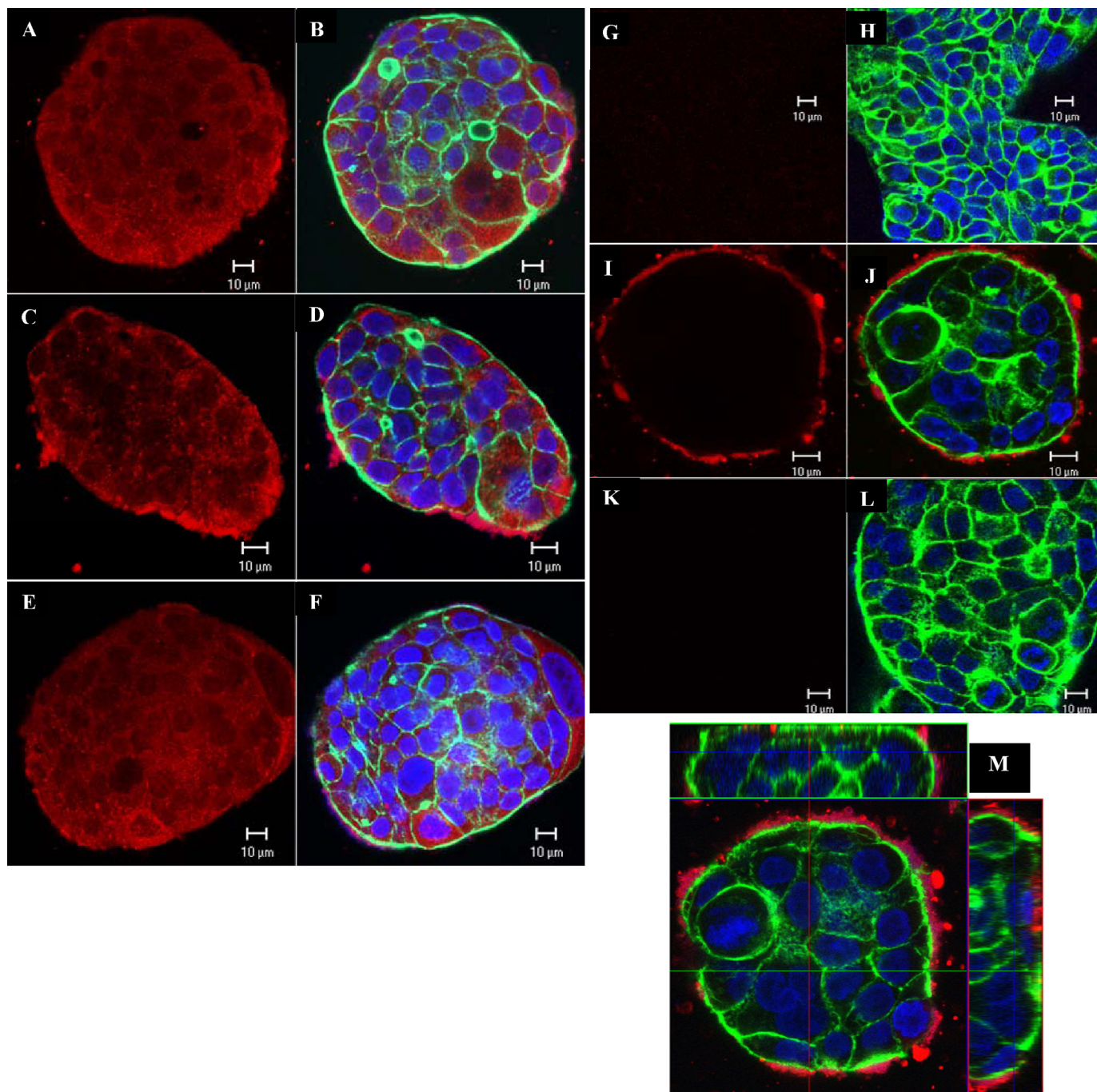
FIGURE 5. **Confocal images of total NIK and phospho-NIK in the NCM460 cells.** In the images of total NIK (*A–F*) and phospho-NIK (*G–L*) actin is stained *green*, DNA is stained *blue*, and NIK or phospho-NIK is stained *red* by fluorescent dyes, as described under "Experimental Procedures." *A* and *B*, total NIK was stained in the control cells. *C* and *D*, total NIK staining after CGN exposure was increased along the cell surface. *E* and *F*, following BCL10 silencing, total NIK staining resembled the distribution seen in the control cells. *G* and *H*, no staining for phospho-NIK was seen in the control cells. *I* and *J*, following CGN exposure, phospho-NIK staining was evident along the outer cell membrane. *K* and *L*, following BCL10 silencing and CGN exposure, no staining for phospho-NIK was evident. *M*, the z-stack confocal image confirms that the phospho-NIK is localized along the cell membrane (x-z and y-z projections).

By induction of both the canonical and noncanonical pathways of NF-κB activation, BCL10 and CGN are positioned to influence a wide range of NF-κB transcriptional effects. The p52/RelB heterodimer appears to bind to a broader spectrum of κB sites than the p50/RelA heterodimer and may even bind to a modified consensus sequence (22–24). By activation of the noncanonical pathway, CGN and BCL10 may evoke responses similar to those of tumor necrosis factor-α, as well as those elicited by inflammatory mediators such as dextran sulfate sodium that act through ROS (17).

The complexity of the negative feedback on NF-κB, involving mediators such as IκBδ, as well as IκB-α, -β, and -ε, may include stimulus specific responses and different, but specified kinetic rate constants (25–28). Also, the protein content of RelB was reported to be significantly reduced when p105 and p100 were absent, suggesting that the noncanonical pathway may be
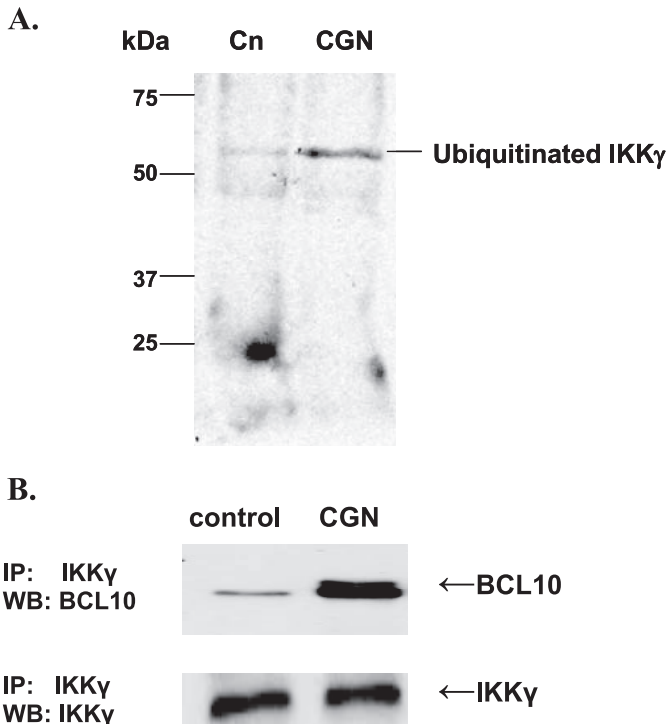
A.

B.

FIGURE 6. **CGN increases IKKγ ubiquitination, and IKKγ co-immunopre-cipitates with BCL10 in NCM460 cells.** *A*, following exposure to CGN in the NCM460 cells, ubiquitination of IKKγ increased, as demonstrated in a representative Western blot (*WB*), following immunoprecipitation (*IP*) with ubiquitin and immunoblotting with IKKγ. *B*, IKKγ co-immunoprecipitated with BCL10, and following CGN exposure, there was marked increase in the BCL10 associated with IKKγ. *Cn*, control.
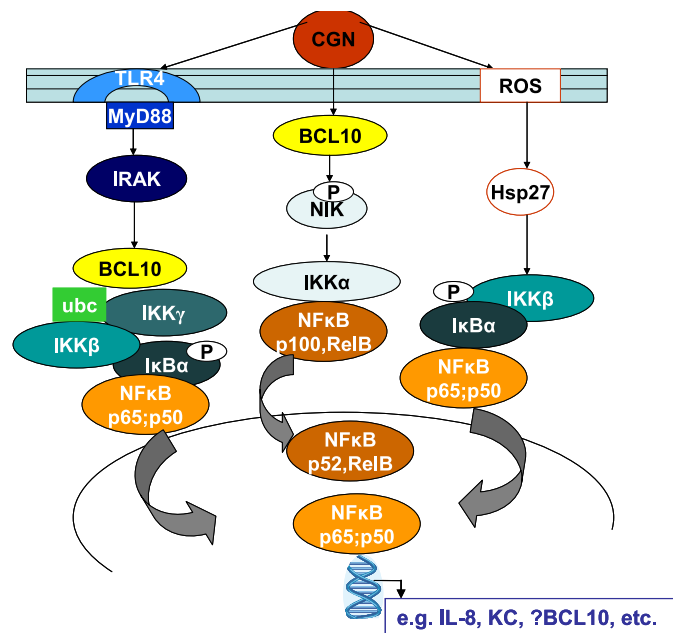

FIGURE 7. **Schematic of overall pathways of IL-8 activation by CGN in NCM460 cells.** Carrageenan activates two major pathways of IL-8 activation: the TLR4-BCL10 pathway and the ROS-Hsp27 mediated pathway. These converge at the level of the IKK signalosome, in which effects on IKKα, -β, and -γ are integrated. Subsequently, in the NCM460 cells, members of the NF-κB family are activated, including p65 (RelA), p50, p100, p52, and RelB. The activation of phospho-NIK was repressed by BCL10 silencing. *IRAK*, interleukin-1 receptor-associated kinase; *ubc*, ubiquitin c; *p*, phosphorylated.

affected by intricate protein-protein relationships that exist among NF-κB components, as well as by transcriptional events. The interaction of these regulatory mechanisms with BCL10 poses an additional series of mechanistic interactions that require further investigation.

The study findings demonstrated an increase in phospho-NIK following stimulation by CGN and showed localization of phospho-NIK to the outer cell membrane. BCL10 silencing inhibited the CGN-induced effects on phospho-NIK. These data challenge some previous observations about NIK activation, because previously, the LPS-activated TLR-mediated pathway was not associated with NIK (29), and we have found that the TLR4-BCL10 mediated pathway resembles the CGN-activated pathway (16). The data demonstrated that BCL10 silencing inhibited the increase in phospho-NIK, consistent with a vital role for BCL10 in the IKKα-mediated pathway, although the role of phospho-NIK in the IKKβ-mediated pathway remains obscure.

The translocation of phospho-NIK to the outer cell membrane was unexpected but resembles changes shown upon activation of other molecules, including the catalytic subunit of $(Na^+ + K^+)$-ATPase and sphingosine kinase (SphK1) (30, 31). SphK1 translocation to the plasma membrane from the cytosol involved activation of G(q)-coupled receptors, stimulation by platelet-derived growth factor, nerve growth factor, insulin-like growth factor, tumor necrosis factor-α, IgE, lysophosphatidic acid, or methacholine, and phosphorylation of Ser^{225}. The phenomenon of "signaling inside out" has been associated with the SphK1 translocation, leading to the secretion of sphingosine-1-phosphate with subsequent cross-activation of sphingosine-1-phosphate G-protein-coupled receptors. No evidence exists at this time for involvement of G-protein-coupled receptor signaling or altered signaling dynamic of pNIK, although the SphK1 paradigm is provocative in consideration of how a localized stimulus can propagate. Altered cellular localization of pNIK following activation of NIK was observed previously in renal tubular cells from tissue preparations in models of ischemia-reperfusion (32). The distinct localization along the outer surface of the cells is attributable to the large size of the carrageenan molecule, limiting its direct effect to cells on the surface, as noted previously with the CGN-TLR4 interaction (9).

Vital questions remain regarding BCL10 interactions with other known mediators of inflammatory mechanisms in both immune and nonimmune cells. The CBM complex, comprised of Carma1 (CARD 11) or Carma3 (CARD 10), BCL10, and MALT1, has been identified as critical to propagation of the inflammatory stimulation, yet the precise mechanism of the CARD-CARD interaction between CARMA and BCL10 and the relationship to MALT1 and other mediators require further elucidation of the precise protein-protein interactions involved. In addition, other important mediators of the inflammatory cascade(s), including TRAFs 2, 3, 4, and 6, TAB1 and 2, as well as RIP, are intimately involved in the cellular inflammatory response, yet their activating or regulating functions with regard to BCL10 require further investigation. Interestingly, BCL10 silencing does not inhibit the effects of tumor necrosis factor-α (15), implying that there may be multiple upstream mechanisms by which NIK is activated prior to interaction with

IKKα. This combination of specificity and redundancy is consistent with a somewhat limited repertoire of cellular inflammatory responses to a more unlimited variety of extracellular stimuli that are integrated at the level of the IKK signalosome.

Recent findings in our lab indicate that the BCL10 promoter contains a sequence that has a very high score (>90%) for likelihood as an NF-κB binding site (33). This suggests the possibility that CGN may induce the constitutive activation of a BCL10/NF-κB loop, in which increases in BCL10 lead to increases in NF-κB and increases in NF-κB lead to increases in BCL10. This may lead to an ongoing cycle of inflammation, perhaps autonomous once initiated. Previously, in the MALT lymphomas, constitutive activation of NF-κB arose following chromosomal translocations that affected BCL10 (1, 2). In the setting of exogenous stimulation by CGN, it is possible that constitutive activation of NF-κB and BCL10 follows stimulation due to specific characteristics of the CGN related to its chemical structure, rather than to effects of a specific activating translocation.

Recent publications demonstrate intense interest in the CBM complex in epithelial and endothelial, as well as immune cells (34–38), and increased attention to BCL10 and other CARD proteins may lead to enhanced understanding of these important inflammatory mechanisms. Also, because CGN has been so widely incorporated into a variety of foods in the Western diet, exposure to CGN may have a role in human disease, involving activation of inflammation through the BCL10-mediated pathways.

REFERENCES

1. Zhang, Q., Siebert, R., Yan, M., Hinzmann, B., Cui, X., Xue, L., Rakestraw, K. M., Naeve, C. W., Beckmann, G., Weisenburger, D. D., Sanger, W. G., Nowotny, H., Vesely, M., Callet-Bauchu, E., Salles, G., Dixit, V. M., Rosenthal, A., Schlegelberger, B., and Morris, S. W. (1999) *Nat. Genet.* **22,** 63–68
2. Willis, T. G., Jadayel, D. M., Du, M. Q., Peng, H., Perry, A. R., Abdul-Rauf, M., Price, H., Karran, L., Majekodunmi, O., Wlodarska, I., Pan, L., Crook, T., Hamoudi, R., Isaacson, P. G., and Dyer, J. F. (1999) *Cell* **96,** 35–45
3. Klemm, S., Zimmermann, S., Peschel, C., Mak, T. W., and Ruland, J. (2007) *Proc. Natl. Acad. Sci. U.S.A.* **104,** 134–138
4. Wang, D., You, Y., Lin, P. C., Xue, L., Morris, S. W., Zeng, H., Wen, R., and Lin, X. (2007) *Proc. Natl. Acad. Sci. U.S.A.* **104,** 145–150
5. McAllister-Lucas, L. M., Ruland, J., Siu, K., Jin, X., Gu, S., Kim, D. S., Kuffa, P., Kohrt, D., Mak, T. W., Nuñez, G., and Lucas, P. C. (2007) *Proc. Natl. Acad. Sci. U.S.A.* **104,** 139–144
6. Borthakur, A., Bhattacharyya, S., Dudeja, P. K., and Tobacman, J. K. (2007) *Am. J. Physiol. Gastrointest. Liver Physiol.* **292,** G829–38
7. Bhattacharyya, S., Borthakur, A., Dudeja, P. K., and Tobacman, J. K. (2008) *J. Nutr.* **138,** 469–475
8. Bhattacharyya, S., Dudeja, P. K., and Tobacman, J. K. (2008) *Biochim. Biophys. Acta* **1780,** 973–982
9. Bhattacharyya, S., Gill, R., Chen, M. L., Zhang, F., Linhardt, R. J., Dudeja, P. K., and Tobacman, J. K. (2008) *J. Biol. Chem.* **283,** 10550–10558
10. Bhattacharyya, S., Liu, H., Zhang, Z., Jam, M., Dudeja, P. K., Michel, G., Linhardt, R. J., and Tobacman, J. K. (2009) *J. Nutr. Biochem.* Epub ahead of print
11. Galili, U. (2005) *Immunol. Cell Biol.* **83,** 674–686
12. Moyer, M. P., Manzano, L. A., Merriman, R. L., Stauffer, J. S., and Tanzer, L. R. (1996) *In Vitro Cell. Dev. Biol. Anim.* **32,** 315–317
13. Li, Z. W., Chu, W., Hu, Y., Delhase, M., Deerinck, T., Ellisman, M., Johnson, R., and Karin, M. (1999) *J. Exp. Med.* **189,** 1839–1845
14. Hu, Y., Baud, V., Delhase, M., Zhang, P., Deerinck, T., Ellisman, M., Johnson, R., and Karin, M. (1999) *Science* **284,** 316–320
15. Bhattacharyya, S., Pant, N., Dudeja, P. K., and Tobacman, J. K. (2007) *J. Immunoassay Immunochem.* **28,** 173–188
16. Bhattacharyya, S., Borthakur, A., Pant, N., Dudeja, P. K., and Tobacman, J. K. (2007) *Am. J. Physiol. Gastrointest. Liver Physiol.* **293,** G429–437
17. Bhattacharyya, S., Dudeja, P. K., and Tobacman, J. K. (*2009) Inflamm Bowel Dis.* **15,** 673–683
18. Zhou, H., Wertz, I., O'Rourke, K., Ultsch, M., Seshagiri, S., Eby, M., Xiao, W., and Dixit, V. M. (2004) *Nature* **427,** 167–171
19. Drew, D., Shimada, E., Huynh, K., Bergqvist, S., Talwar, R., Karin, M., and Ghosh, G. (2007) *Biochemistry* **46,** 12482–12490
20. Yilmaz, Z. B., Weih, D. S., Sivakumar, V., and Weih, F. (2003) *EMBO J.* **22,** 121–130
21. Endo, T., Nishio, M., Enzler, T., Cottam, H. B., Fukuda, T., James, D. F., Karin, M., and Kipps, T. J. (2007) *Blood* **109,** 703–710
22. Fusco, A. J., Huang, D. B., Miller, D., Wang, V. Y., Vu, D., and Ghosh, G. (2009) *EMBO Rep.* **10,** 152–159
23. Wharry, C. E., Haines, K. M., Carroll, R. G., and May, M. J. (2009) *Cancer Biol. Ther.* **8,** 1567–1576
24. Dejardin, E. (2006) *Biochem. Pharmacol.* **72,** 1161–1179
25. Shih, V. F., Kearns, J. D., Basak, S., Savinova, O. V., Ghosh, G., and Hoffmann, A. (2009) *Proc. Natl. Acad. Sci. U.S.A.* **106,** 9619–9624
26. Savinova, O. V., Hoffmann, A., and Ghosh, G. (2009) *Mol. Cell.* **34,** 591–602
27. Basak, S., Shih, V. F., and Hoffmann, A. (2008) *Mol. Cell. Biol.* **28,** 3139–3150
28. Smith, C., Andreakos, E., Crawley, J. B., Brennan, F. M., Feldmann, M., and Foxwell, B. M. (2001) *J. Immunol.* **167,** 5895–5903
29. Fusco, A. J., Savinova, O. V., Talwar, R., Kearns, J. D., Hoffmann, A., and Ghosh, G. (2008) *J. Biol. Chem.* **283,** 12324–12332
30. Myers, A. C., Bochner, B. S., Tomaselli, G. F., Fedarko, N., Hudson, S. A., Rohde, H., Huang, S. K., and Xu, K. Y. (2002) *Biochem. Biophys. Res. Commun.* **291,** 111–115
31. ter Braak, M., Danneberg, K., Lichte, K., Liphardt, K., Ktistakis, N. T., Pitson, S. M., Hla, T., Jakobs, K. H., and Zu Heringdorf, D. M. (2009) *Biochim. Biophys. Acta* **1791,** 357–370
32. Loverre, A., Ditonno, P., Crovace, A., Gesualdo, L., Ranieri, E., Pontrelli, P., Stallone, G., Infante, B., Schena, A., Di Paolo, S., Capobianco, C., Ursi, M., Palazzo, S., Battatglia, M., Selvaggi, F. P., Schena, F. P., and Grandaliano, G. (2004) *J. Am. Soc. Nephrol.* **15,** 2675–2686
33. Borthakur, A., Bhattacharyya, S., Alrefai, W., Tobacman, J., Ramaswamy, K., and Dudeja, P. K. (2009) *Inflam. Bowel Dis.* Aug 27, Epub ahead of print
34. Evans, S. E., Scott, B. L., Clement, C. G., Larson, D. T., Kontoyiannis, D., Lewis, R. E., Lasala, P. R., Pawlik, J., Peterson, J. W., Chopra, A. K., Klimpel, G., Bowden, G., Hook, M., Xu, Y., Tuvim, M. J., and Dickey, B. F. (2009) *Am. J. Respir. Cell Mol. Biol.* Mar 27, Epub ahead of print
35. Chang, H. H., Kuo, M. Y., Cheng, S. J., and Chiang, C. P. (2009) *Oral Oncol.* **45,** 589–593
36. Martin, D., Galisteo, R., and Gutkind, J. S. (2009) *J. Biol. Chem.* **284,** 6038–6042
37. Wu, C. J., and Ashwell, J. D. (2008) *Proc. Natl. Acad. Sci. U.S.A.* **105,** 3023–3028
38. Briones, J., Moga, E., Espinosa, I., Vergara, C., Alvarez, E., Villa, J., Bordes, R., Delgado, J., Prat, J., and Sierra, J. (2009) *Histopathology* **54,** 478–485